RAFT Polymerization | Hot Paper |

Switchable Electrostatically Templated Polymerization

Chendan Li, Jose R. Magana, Fabian Sobotta, Junyou Wang, Martien A. Cohen Stuart,
Bas G. P. van Ravensteijn,* and Ilja K. Voets*

Abstract: We report a switchable, templated polymerization system where the strength of the templating effect can be modulated by solution pH and/or ionic strength. The responsiveness to these cues is incorporated through a dendritic polyamidoamine-based template of which the charge density depends on pH. The dendrimers act as a template for the polymerization of an oppositely charged monomer, namely sodium styrene sulfonate. We show that the rate of polymerization and maximum achievable monomer conversion are directly related to the charge density of the template, and hence the environmental pH. The polymerization could effectively be switched "ON" and "OFF" on demand, by cycling between acidic and alkaline reaction environments. These findings break ground for a novel concept, namely harnessing co-assembly of a template and growing polymer chains with tunable association strength to create and control coupled polymerization and self-assembly pathways of (charged) macromolecular building blocks.

[*] C. Li, J. Wang, M. A. C. Stuart
State Key Laboratory of Chemical Engineering and Shanghai Key Laboratory of Multiphase Materials Chemical Engineering
East China University of Science and Technology
130 Meilong Road, Shanghai 200237 (P. R. China)

C. Li, J. R. Magana, F. Sobotta, B. G. P. van Ravensteijn, I. K. Voets
Institute for Complex Molecular Systems, Department of Chemical Engineering and Chemistry, Eindhoven University of Technology
P.O. Box 513, 5600 MB Eindhoven (The Netherlands)
E-mail: b.g.p.vanravensteijn@uu.nl
i.voets@tue.nl

J. R. Magana
Current address: Grup d'Enginyeria de Materials (GEMAT), Institut Químic de Sarrià (IQS), Universitat Ramon Llull (URL)
08022 Barcelona (Spain)

B. G. P. van Ravensteijn
Current address: Department of Pharmaceutics, Utrecht Institute for Pharmaceutical Sciences (UIPS), Faculty of Science, Utrecht University
P.O. Box 80082, 3508 TB Utrecht (The Netherlands)

Introduction

Templated polymerizations make use of (macro)molecular blueprints for the synthesis of new macromolecules.[1] Properties such as tacticity, molecular weight (distribution), polymer topology, and monomer sequence are transferred from the template to the newly synthesized polymers. Arguably the most significant example of these templated polymerizations are the transcription and translation steps involved in the fabrication of proteins as prescribed by the DNA code and enabled by RNA intermediates.[2] In synthetic systems, combining free-radical, controlled radical, condensation, and ring-opening (co)polymerization with templates produces, for example, cyclic polymers, (semi-)ladder polymers, and one-pot blocky macromolecules that cannot be attained by traditional means.[1,3–12] Recruitment by and pre-organization of monomers and growing chains on the template can be achieved in many ways, e.g., by hydrogen bonds, electrostatic forces, or covalent bonds.

Although originally focused on transferring molecular information, more recently, electrostatically-driven templated polymerizations were also used as means to direct the assembly of macromolecular building blocks. In these so-called polymerization-induced electrostatic self-assembly (PIESA) or electrostatic assembly-directed polymerization (EADP) procedures, neutral-polyelectrolyte block copolymers are being synthesized in the presence of oppositely charged templates.[13–18] At a certain block length, the charged components phase separate and become strongly enriched in a condensed state. The neutral block restricts the phase separation to nanoscopic length scales, generating micelles, vesicles and other nanoparticles. The sizes and shapes of these assemblies are dictated by the block-length ratio, molecular weight, total polymer content, salt concentration, and polymerization kinetics.[19–21] The latter offers a convenient handle to prepare distinctly different nanoparticles from the same building blocks. Since both thermodynamic and kinetic parameters impact particle shape and size, these tend to differ from what one would obtain by simply mixing the preformed block-copolymers and the template. In this respect, PIESA is reminiscent of polymerization-induced self-assembly (PISA) methods, which rely on the in situ generation of amphiphilic macromolecular building blocks that assemble into higher-order structures with morphologies dictated by the time-dependent amphiphilic balance of the forming polymers.[22–24] Including secondary directional interactions, e.g., hydrogen bonds, can be exploited to further gain structural control during the polymerization process.[25] However, the direct interaction of

the growing polymers with the template in PIESA adds an extra layer of complexity to these dynamic self-assembling systems. The fundamental understanding of the effect of macromolecular scaffolds and how these interact with the monomers and growing polymers is pivotal, but up-to-date insufficient to produce predictable colloidal structures.[15]

Here, we contribute to this open challenge by presenting and exploring an electrostatically templated polymerization system wherein the strength of the templating effect can be modulated by external cues, e.g., ionic strength and solution pH. The tunability originates from a template that carries a pH-dependent cationic charge density. By controlling the solution pH, and hence the template's degree of protonation, we gain control over the polymerization kinetics of an oppositely charged monomer (sodium styrene sulfonate (NaSS)). Furthermore, the polymerization could be switched "ON" and "OFF" reversibly by simply toggling between acidic and alkaline reaction conditions. The presented system unlocks new avenues in devising coupled polymerization and assembly pathways, beyond what has been achieved with non-switchable templates. To substantiate this, we show that in situ and on demand modulation of the templating strength has a distinct influence on the characteristics of the obtained macromolecular assemblies, unequivocally underlining the importance of controlling assembly pathways.

Results and Discussion

The polymerization system investigated here comprises generation 3 polyamidoamine (PAMAM) dendrimers as "switchable" templates. These molecularly-defined macromolecules contain primary amines and two populations of tertiary amines that can be protonated depending on the environmental pH (Scheme 1).[27] When in the protonated form, the amines are positively charged. Considering the significantly different pK_a values for primary and tertiary amines, the overall charge density of the PAMAM dendrimers is widely tunable over a broad pH range. Aiming to exploit this pH-dependent charge density to modulate template-binding and thereby polymerization of oppositely charged monomers, we selected sodium NaSS as monomer since it carries a negative charge regardless of the environmental pH. For this template and monomer pair, the templating effect should be directly related to the strength of the ionic bonds formed between them.

Polymerizations were performed in aqueous media via a photo-induced reversible addition-fragmentation chain-transfer (RAFT) polymerization using a poly(N-isopropylacrylamide) (p(NIPAM)-based chain transfer agent (macroCTA, degree of polymerization, $DP_n = 200$, $M_{n,SEC} = 26800\ \mathrm{g\,mol^{-1}}$, $Đ = 1.16$, $M_{n,peak,MALDI} = 23600\ \mathrm{g\,mol^{-1}}$; see Supporting Information S2). 2-Hydroxy-2-methylpropiophenone (HMPP) was added as a light-sensitive radical source, enabling the polymerization to run at room temperature. Under appropriate RAFT polymerization
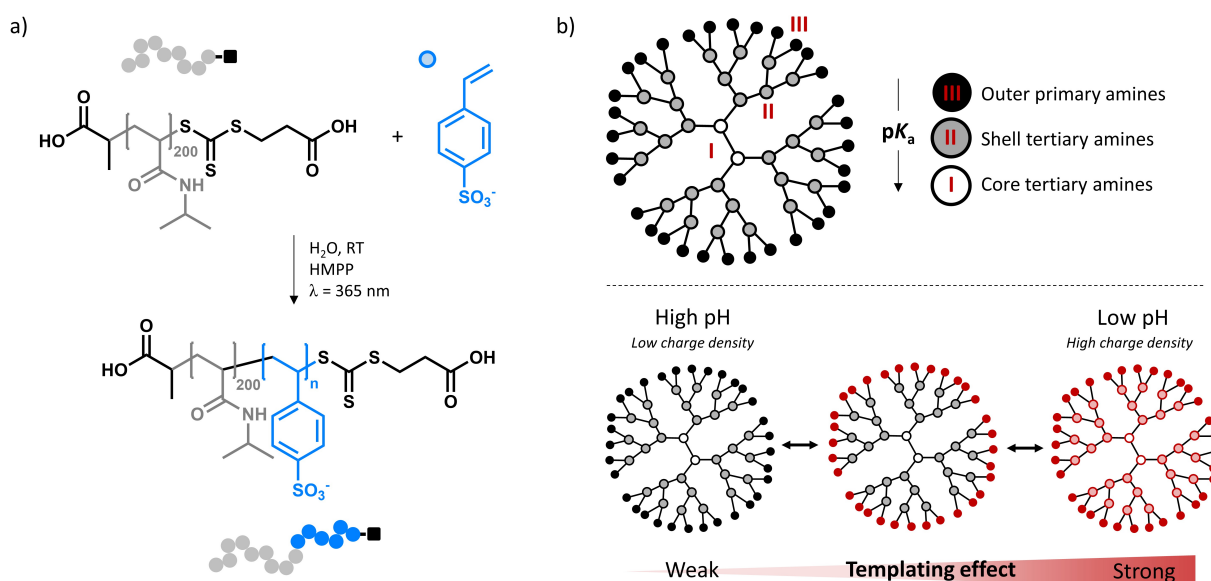
Scheme 1. a) Schematic overview of the photo-induced reversible addition-fragmentation chain-transfer (RAFT) of sodium styrene sulfonate (NaSS, blue) polymerization using a poly(N-isopropylacrylamide) (p(NIPAM)-based chain transfer agent (macroCTA, degree of polymerization, $DP_n = 200$, grey). 2-Hydroxy-2-methylpropiophenone (HMPP) was added as a light-sensitive radical source. Polymerizations were conducted in buffered aqueous media at room temperature under LED illumination ($\lambda_{max} = 365\ \mathrm{nm}$). The reaction yields block copolymers with a charge-neutral p(NIPAM) and permanently negatively charged p(SS) segment (p(NIPAM-b-SS). b) Pictorial depiction of the generation 3 polyamidoamine (PAMAM) dendritic template. The template contains primary amines (**III**) and two populations of tertiary amines (**II, I**). The pK_a of these amines decreases when moving from the periphery of the molecule radially inwards. The differences in pK_a enable to regulate the charge density of the dendrimers with pH. At high pH, the dendrimers carry little to no charge. In this state the templating effect for the NaSS polymerization is weak or absent. At low pH, the charge density of PAMAM is high and the dendrimers can act as a template for NaSS.

conditions, the added monomer grows preferentially from the CTA.[26] Because a macromolecular CTA was selected, polymerizing NaSS generates poly(*N*-isopropylacrylamide-*b*-styrene sulfonate) (p(NIPAM-*b*-SS)) block copolymers (Scheme 1, see Supporting Information S4 for diffusion-order spectroscopy nuclear magnetic resonance (DOSY NMR) results to support block copolymer formation). These block copolymers were targeted to constrain the assembly of the template and the oppositely charged polystyrene sulfonate (p(SS)) to the colloidal domain. Targeting an average DP_n of 50 for the p(SS) segment, ensures that the charge-neutral and hydrophilic p(NIPAM) segments of the forming p(NIPAM-*b*-SS) block copolymers are long enough to provide sufficient steric stabilization of the complex coacervate core, essentially forcing the polymers to form micellar clusters of colloidal dimensions.[19] The NaSS and PAMAM concentration were chosen such that the concentration of chargeable amines was equal to the sulfonate concentration (5 mM), i.e., when PAMAM is fully charged, the system operates under charge-neutral conditions. It was verified that when templating was fully suppressed no polymerization occurred over the course of 24 h at such low monomer concentrations. This was realized either in the absence of the PAMAM template (Figure 1a, yellow circles), or upon polymerization under strongly alkaline conditions (pH = 11) were PAMAM carries no charge (Figure 1a, black downward triangles). We would like to emphasize that suppression of polymerization is not caused by irreversible aminolysis of the CTA end groups of the p(NIPAM)-derived macroCTA, as no chain end degradation was observed under the applied reaction conditions over the course of 4 h (see Supporting Information S3). In contrast, lowering the pH to maximize PAMAM's charge density via protonation of the primary and tertiary amines (pH = 3, 20 mM glycine buffer), resulted in fast polymerization of the NaSS monomer (Figure 1a, red squares). A maximum conversion of approximately 93 % was attained after 60 min, as determined by ^{1}H-NMR spectroscopy. The significant increase in polymerization rate (R_p) is directly related to the binding of the NaSS to the charged template which implies a local increase in monomer concentration. The binding of the monomer was evident from broadening or even disappearance of the otherwise sharp NaSS NMR signals caused by a pronounced decrease in molecular reorientation rate.[15] Note that the NMR samples used for conversion measurements were alkalized or salted by addition of 100 mM NaCl before recording the spectrum; this serves to release all monomers from the template and obtain a reliable measure of the concentration of unreacted monomers (see Supporting Information S5). To further confirm that the template-monomer interactions were governed by electrostatics, a polymerization at low pH, but elevated ionic strength was performed. The added salt (NaCl, 100 mM) effectively lowers the local monomer concentration as it screens the charges on PAMAM and NaSS. As anticipated, weakening the templating effect results in slower polymerization kinetics (Figure 1b, grey upright triangles). In agreement with previously reported kinetic data on templated controlled radical polymerization, the reaction shows first-order kinetics pointing to a constant radical concentration throughout the reaction and hence a controlled chain growth process.

Finer control over the polymerization speed could be obtained by performing the reaction at pH values intermediate to the completely "OFF" (pH = 11) and fully "ON" (pH = 3) states, namely pH = 5, 7, and 9 (Figure 2b). All reactions were performed under buffered conditions to prevent the pH from drifting during the polymerization. R_p, reflected by the slope of the semilogarithmic plots, scales with the degree of template protonation. Additionally, the
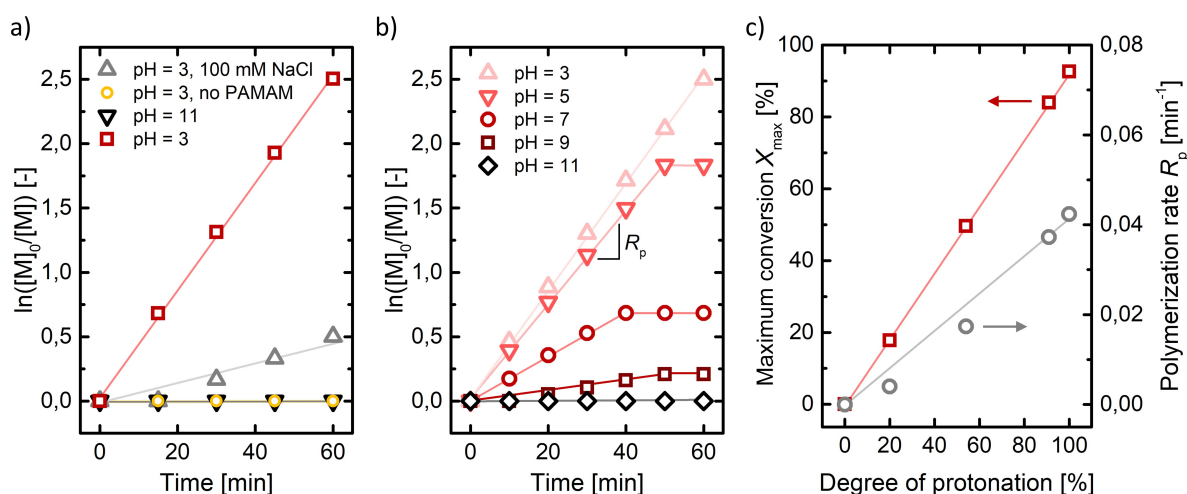

Figure 1. a) Semi-logarithmic plot representing the polymerization kinetics of sodium styrene sulfonate (NaSS) in the absence (yellow circles) and presence of the polyamidoamine (PAMAM) template at pH = 3 (red squares), pH = 11 (black downwards triangles), and at pH 3 and 100 mM NaCl (grey upright triangles). b) Semi-logarithmic kinetic plots for the templated polymerization of NaSS at pH = 3 (upright triangle), 5 (downward triangle), 7 (circles), 9 (squares), and 11 (diamonds). The initial slopes of these curves are a measure for the rate of polymerization (R_p). c) Maximum attainable NaSS conversion (X_{max}, red squares) and initial R_p as a function of the degree of template protonation. Degrees of protonation at the given reaction pH values were taken from Ref. [27] (see Supporting Information S6).
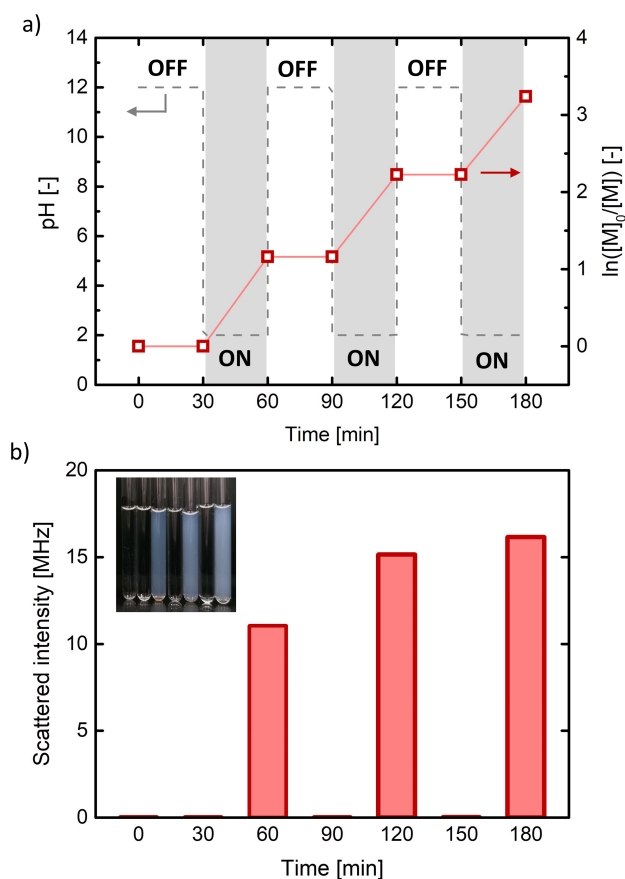
a)

b)

Figure 2. a) Semi-logarithmic plot representing the polymerization kinetics during a templated polymerization that was switched "ON" (highlighted in grey) and "OFF" by addition of acid and base, respectively (red data points; right y-axis). The pH of the reaction mixture throughout the process is depicted by the grey striped curve (left y-axis). b) Time-dependent evolution of the scattered intensity of the "ON"—"OFF" reaction depicted in panel a. Only in the "ON" state, when the formed poly(styrene sulfonate) (p(SS))-containing polymers and the template are bound, significant scattering intensity was measured. The scattered intensity increases with the number of "ON" periods. In the "OFF" state, all macromolecular components are molecularly dissolved resulting in negligible scattering.

maximum attainable monomer conversion (X_{max}) is set by the charge density of PAMAM. Given the fact that only the monomer bound to the template can participate in the polymerization, the reactions undergo self-quenching once the bound population of monomer is depleted. The relation between R_p, X_{max}, and the degree of PAMAM protonation is highlighted in Figure 1c. The degrees of protonation as a function of the solution pH were taken from Cakara et al. (see Supporting Information S6).[27] The linear relation of R_p with respect to the template charge, and hence local monomer concentration, is in line with the first-order reaction kinetics expected for controlled radical polymerizations.

Next, we investigated the reversibility of the templating effect of PAMAM by cycling between high (≥ 12) and low (≤ 2) pH. For these experiments, no buffer was used, enabling the modulation of the pH by addition of aqueous

HCl or NaOH solutions every 30 min. Concentrated HCl or NaOH solutions were used to minimize the effect of dilution. Again, the polymerization kinetics were monitored using ^{1}H-NMR. Figure 2 shows the anticipated "ON"—"OFF" switch behavior, where polymerization only occurs in acidic environments (grey highlighted sections). Whenever the reaction environment was alkaline, the polymerization was completely quenched. Complete and fast suppression of the polymerization is facilitated by the fast release of the template-bound monomer. The semi-logarithmic plots in the low-pH "ON" sections have similar slopes, suggesting that the system immediately resumes the configuration and corresponding reaction control from the previous "ON" section, despite the intermediate "OFF" periods. The moderate build-up of ionic strength per "ON"—"OFF" cycle (≈ 10 mM), proved to be insufficient to significantly slow down the polymerization over the course of 3 cycles. However, the increase in ionic strength imposes an experimental constraint on the number of cycles that can be performed before detrimentally affecting the electrostatically mediated templating effect.

In addition to the NMR data, the progression of the switchable templated polymerization could also be followed by light scattering experiments (Figure 2b). At the start of the polymerization, or when the templating effect is too weak, all components are molecularly dissolved, yielding low scattered intensities. However, under acidic conditions, when the p(SS) segments start to grow and are complexed to the charged PAMAM, larger structures of colloidal dimensions are formed. These objects scatter significantly more light compared to their unassociated building blocks. Obtaining colloidal objects also advocates for the formation of (p(NIPAM-*b*-SS)) block copolymers, in agreement with the previously mentioned DOSY NMR results and the anticipated block ratios between the negatively charged p(SS) segments and the stabilizing p(NIPAM) blocks (Supporting Information S4). If (large fractions) of p(SS) homopolymers would have been formed, electrostatically mediated association would have led to uncontrolled (macroscopic) aggregation. As the number of low-pH "ON" periods increases, the scattered intensity grows, likely due to an increase in particle size, concentration or potentially morphological transitions as the NaSS block grows in length (see Supporting Information S7 for detailed analysis and discussion).[28,29] This growth was also visually evident from the light scattering samples. Only at low pH the samples appear turbid, while fully transparent solutions were obtained in the high-pH "OFF" state. Interestingly, the nanoparticles obtained after the "ON"–"OFF" cycling have a higher light scattering intensity and lower diffusion coefficients (reflecting a larger hydrodynamic size) compared to the assemblies obtained via a continuous polymerization at similar final NaSS conversions (60 min at pH=3) or prepared by simply mixing preformed polymers (Supporting Information S8). This result underlines the importance of the assembly pathway and shows that switchable templates offer control options beyond what has to date been realized with polymerization-induced (electrostatic) self-assembly protocols.
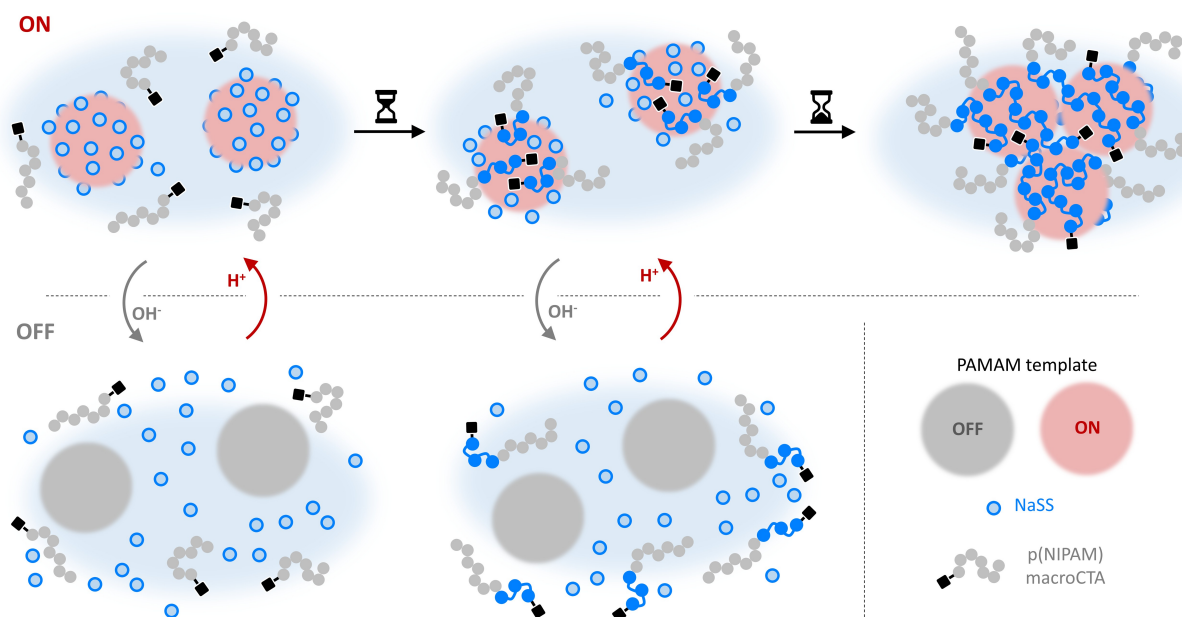
Figure 3. Schematic representation of the switchable templated polymerization concept. At high pH, the system resides in its "OFF" state (bottom row). In this state, the polyamidoamine (PAMAM) template is uncharged (large grey circle). The negatively charged monomer (sodium styrene sulfonate, NaSS, blue open circle) does not feel the presence of the template. Upon lowering the pH, the template is switched on. In this "ON" state (top row), PAMAM is positively charged and NaSS is recruited to the template by means of electrostatic interactions. The monomer recruitment leads to a locally higher monomer concentration that favors polymerization of NaSS controlled by the dissolved poly(*N*-isopropylacrylamide) (p(NIPAM)-based chain transfer agent (macroCTA, grey). At any given point during the reaction, the polymerization can be quenched by switching off the template (middle column). At sufficiently high NaSS conversions, complex core coacervate micelles form.

Conclusion

In summary, we have introduced the concept of switchable templated polymerizations (Figure 3). Making use of a well-defined dendritic template with tunable charge density, the rate of polymerization of an oppositely charge monomer and its maximum achievable conversion could be regulated by simply controlling pH and ionic strength. Electrostatic attraction between the monomer and the template causes a local increase in monomer concentration that enables polymerization at a pH-dependent (first order) rate. As the templating effect relies on non-covalent electrostatic forces, it can be switched "ON" and "OFF" on demand by pH and ionic strength as external triggers. The presented results are not only readily translated to other ionic template–monomer combinations, but also to other non-covalent template–monomer interactions, e.g., hydrogen bonding, metal coordination, or hydrophobic forces, that rely on additional external control factors like temperature or redox potential. Hence, numerous protocols could be employed to steer the assembly pathways and final properties of growing macromolecules. We envision that the ability to modulate the templating effect, and hence the interaction strength between the polymers in situ, opens up new avenues in polymer synthesis and assembly, employing temporal control of the degree of structural rearrangement. Together with tunable polymerization kinetics and the versatility of this templating concept, the library of assembled polymer structures based on a fixed set of building blocks can be further diversified.

Conflict of Interest

The authors declare no conflict of interest.

Data Availability Statement

The data that support the findings of this study are available from the corresponding author upon reasonable request.

[1] S. Połowiński, *Prog. Polym. Sci.* **2002**, *27*, 537–577.

[2] J. M. Berg, J. L. Tymoczko, L. Stryer, *Biochemistry*, W. H. Freeman, San Francisco, **2006**.

[3] R. Saito, *Polymer* **2008**, *49*, 2625–2631.

[4] R. Saito, Y. Okuno, H. Kobayashi, *J. Polym. Sci. Part A* **2001**, *39*, 3539–3546.

[5] X. Li, H. Zheng, B. Gao, Y. Sun, B. Liu, C. Zhao, *Chemosphere* **2017**, *167*, 71–81.

[6] M. G. Cascone, L. Lazzeri, N. Barbani, C. Cristallini, G. Polacco, *Polym. Int.* **1996**, *41*, 17–21.

[7] Y. Chen, X. Li, W. Zizeng, L. Feng, J. Xie, Z. Lin, Z. Xu, B. Liu, X. Li, H. Zheng, *Environ. Sci. Pollut. Res. Int.* **2021**, *28*, 51865–51878.

[8] B. D. Ippel, M. I. Komil, P. A. A. Bartels, S. H. M. Söntjens, R. J. E. A. Boonen, M. M. J. Smulders, P. Y. W. Dankers, *Macromolecules* **2020**, *53*, 4454–4464.

[9] S. Ida, T. Terashima, M. Ouchi, M. Sawamoto, *J. Am. Chem. Soc.* **2009**, *131*, 10808–10809.

[10] S. Ida, M. Ouchi, M. Sawamoto, *Macromol. Rapid Commun.* **2011**, *32*, 209–214.

[11] P. K. Lo, H. F. Sleiman, *J. Am. Chem. Soc.* **2009**, *131*, 4182–4183.

[12] X. Li, Z. Y. J. Zhan, R. Knipe, D. G. Lynn, *J. Am. Chem. Soc.* **2002**, *124*, 746–747.

[13] Q. Zhao, Q. Liu, C. Li, L. Cao, L. Ma, X. Wang, Y. Cai, *Chem. Commun.* **2020**, *56*, 4954–4957.

[14] Q. Liu, X. Wang, L. Ma, K. Yu, W. Xiong, X. Lu, Y. Cai, *ACS Macro Lett.* **2020**, *9*, 454–458.

[15] I. Bos, C. Terenzi, J. Sprakel, *Macromolecules* **2020**, *53*, 10675–10685.

[16] Q. Yu, Q. Ding, H. Cao, X. Lu, Y. Cai, *ACS Macro Lett.* **2015**, *4*, 1293–1296.

[17] Y. Ding, Q. Zhao, L. Wang, L. Huang, Q. Liu, X. Lu, Y. Cai, *ACS Macro Lett.* **2019**, *8*, 943–946.

[18] P. Ding, L. Chen, C. Wei, W. Zhou, C. Li, J. Wang, M. Wang, X. Guo, M. A. Cohen Stuart, J. Wang, *Macromol. Rapid Commun.* **2021**, *42*, 2000635.

[19] I. K. Voets, A. de Keizer, M. A. Cohen Stuart, *Adv. Colloid Interface Sci.* **2009**, *147–148*, 300–318.

[20] A. E. Marras, J. M. Ting, K. C. Stevens, M. V. Tirrell, *J. Phys. Chem. B* **2021**, *125*, 7076–7089.

[21] C. C. M. Sproncken, J. R. Magana, I. K. Voets, *ACS Macro Lett.* **2021**, *10*, 167–179.

[22] J. Cao, Y. Tan, Y. Chen, L. Zhang, J. Tan, *Macromol. Rapid Commun.* **2021**, *42*, 2100498.

[23] F. D'Agosto, J. Rieger, M. Lansalot, *Angew. Chem. Int. Ed.* **2020**, *59*, 8368–8392; *Angew. Chem.* **2020**, *132*, 8444–8470.

[24] N. J. W. Penfold, J. Yeow, C. Boyer, S. P. Armes, *ACS Macro Lett.* **2019**, *8*, 1029–1054.

[25] G. Mellot, J.-M. Guigner, L. Bouteiller, F. Stoffelbach, J. Rieger, *Angew. Chem. Int. Ed.* **2019**, *58*, 3173–3177; *Angew. Chem.* **2019**, *131*, 3205–3209.

[26] S. Perrier, *Macromolecules* **2017**, *50*, 7433–7447.

[27] D. Cakara, J. Kleimann, M. Borkovec, *Macromolecules* **2003**, *36*, 4201–4207.

[28] H. M. Van Der Kooij, E. Spruijt, I. K. Voets, R. Fokkink, M. A. Cohen Stuart, J. Van Der Gucht, *Langmuir* **2012**, *28*, 14180–14191.

[29] S. Van Der Burgh, A. De Keizer, M. A. Cohen Stuart, *Langmuir* **2004**, *20*, 1073–1084.